J. Membrane Biol. 148, 143–156 (1995)

The Journal of
Membrane
Biology

Patch Clamp Study of the Voltage-dependent Anion Channel in the Thylakoid Membrane

I.I. Pottosin,[1] G. Schönknecht[2]

[1]Institute for Cell Biophysics, Russian Academy of Sciences, 142292 Puschino, Moscow region, Russia
[2]Julius-von-Sachs Institut für Biowissenschaften der Universität Würzburg, Mittlerer Dallenbergweg 64, D-97082 Würzburg, Germany

Received: 4 May 1995/Revised: 24 July 1995

Abstract. Measurements of single channel currents were performed on isolated membrane patches from osmotically swollen thylakoids of the Charophyte alga *Nitellopsis obtusa.* A channel with a high selectivity for anions over cations and a conductance of 100 to 110 pS (114 mM Cl^-) was revealed. The channel has a bell-shaped voltage-dependence of the open probability, with a maximum at about 0 mV. This dependence was explained by two gating processes, one causing channel closure at positive and one at negative potentials. The steepness of the voltage-dependence corresponded to approximately 2 elementary charges to be transferred across the entire membrane in each of the two gating processes. The analysis of the anion channel kinetics in the millisecond time domain revealed an e-fold increase of mean open and decrease of mean closed times when the membrane voltage was made more positive by 20 and 36 mV, respectively. Concert transitions of two identical anion channels between open and long inactivated states were observed, while the millisecond closed-open transitions of the two channels within a burst of activity were kinetically independent.

Key words: Anion channel — Channel gating — Patch-clamp — Thylakoid membrane — *Nitellopsis obtusa*

Introduction

Light-driven electron transfer across the photosynthetic (thylakoid) membrane of higher plants and algae is coupled to H^+ uptake into the thylakoid lumen. As a result, a transmembrane electrochemical gradient for protons is built up which is used by thylakoid H^+-ATPase for ATP synthesis. Unlike in bacterial chromatophores and mitochondria, this gradient ($\Delta\mu H$) is largely chemical (ΔpH), while the electrical potential difference is close to zero at steady state (Bulychev et al., 1972; Rottenberg, Grunwald & Avron, 1972; Junge & Jackson, 1982; Remiš, Bulychev and Kurella, 1986). A massive electroneutral uptake of protons in the light is possible due to a counterflow of other ions across the thylakoid membrane. Both uptake of Cl^- and efflux of K^+ and Mg^{2+} have been shown to balance electrically the *net* H^+ influx (Dilley & Vernon, 1965; Deamer & Packer, 1969; Hind, Nakatani & Izawa, 1974; Bulychev & Vredenberg, 1976; Vambutas & Schechter, 1983).

Several attempts were made to characterize the ion-transport pathways in thylakoid membranes directly by means of electrophysiological techniques. First, a 110 pS channel, highly selective for anions, was revealed by patch-clamping osmotically inflated thylakoids of a higher plant *Peperomia metallica* (Schönknecht et al., 1988). Upon reconstitution of spinach thylakoid membranes into planar lipid bilayers (Tester & Blatt, 1989) or into giant liposomes (Enz, Steinkamp & Wagner, 1993), cation-selective channels have been found.

In this study we have analyzed ion channels of the intact thylakoid membrane of a Charophyte alga (*Nitellopsis obtusa*) by the patch clamp technique.

Materials and Methods

Plant material: Cells of *Nitellopsis obtusa* were collected in Valdai lake (Novgorod region, Russia) and kept under room temperature (20–25°C) and day light conditions in a 30 dm^3 aquarium filled with distilled water and quartz sand.

Preparation

Intact chloroplasts were isolated mechanically. The isolation procedure for *Nitellopsis obtusa* was described elsewhere (Pottosin, 1992).

Correspondence to: I.I. Pottosin

Briefly, a giant alga cell was gently dried by filter paper and immersed in a solution containing (in mM): 100 KCl, 100 sorbitol, 2 $CaCl_2$, 5 $MgCl_2$, 1 EDTA, 10 HEPES-KOH, pH 7.5 ("100 KCl" solution). Both cell ends were cut off, the cell sap was squeezed from the cell, and an aliquot of this solution containing chloroplasts was transferred into the experimental chamber containing the same suspending medium.

When the chloroplasts have stuck to the bottom of experimental chamber the solution in the chamber was replaced by a hypotonic one containing (in mM): 15 KCl, 2 $CaCl_2$, 5 $MgCl_2$, 1 EDTA, 10 HEPES-KOH, pH 7.5 ("15 KCl" solution). This caused rupture of the chloroplast envelope and swelling of thylakoid membranes. Usually, within 5 minutes large (10–15 μm) spherical blebs formed by swollen thylakoid membrane were observed and used for patch-clamp recordings.

Patch-Clamp Measurements

Micropipettes were made from Kimax-51 glass (Witz Scientific, Ohio) by two steps pulling (L/M-3P-A puller, List-Medical, Darmstadt, Germany). After fire polishing (L/M-CPZ-101, List-Medical) the resistance of the electrode filled with "15 KCl" solution was 20–25 MΩ (*cf.* 10–12 MΩ when filled with "100 KCl" solution). The "15 KCl" solution (filtered through a 0.2 μm filter) was used routinely as electrode filling solution, while bath solution contained 15, 100 or 200 mM KCl, *see* figure legends for details. The reference AgCl electrode was connected to the chamber by an agar bridge filled with 100 mM KCl. The offset potential was corrected at the beginning of each experiment and was tested at the end, after breakdown of the patch (drift <2 mV).

Electrical measurements were performed using an Axopatch 200A Integrating Patch-Clamp amplifier (Axon Instruments, Foster City). Tight seals (2–10 GΩ) between glass microelectrode and thylakoid membrane were achieved by applying a slight suction pulse. All experiments were performed in the inside-out patch configuration (Hamill et al., 1981). The convention of current and voltage is according to Azzone et al. (1993), i.e., the sign of voltage was determined as stromal *minus* thylakoid lumen side. Positive currents represent an efflux of cations from the pipette into the intrathylakoid side or an anion influx from the lumen side into the pipette. The records were filtered at 10 kHz by a low pass Bessel filter, were digitized using a VR-10B digital data recorder (Instrutech Corp., New York) and stored on videotape. For the analysis selected records were filtered and transferred to IBM-compatible PC, *see* figure legends for filter cutoff frequency and sampling rate. The analyses were carried out using the pClamp 6.0 software package (Axon Instruments).

Results

General Observations

There is one report about successfully patch clamping swollen thylakoid membranes (Schönknecht et al., 1988). However, this approach is not a routine one. Other research groups did not reproducibly achieve high resistance seals in the GΩ range between the glass microelectrode and the thylakoid membrane (Enz et al., 1993). The major reasons for these difficulties might be the unusual high protein to lipid ratio and the large surface charge of thylakoid membranes. Therefore, we first had to elaborate an optimum procedure for obtaining GΩ seals with thylakoid membranes.

The optimum characteristics of patch clamp pipettes and composition of solutions were as described in Materials and Methods. It should be noted that a high concentration of divalent cations in the bath was important. When instead of 2 mM $CaCl_2$ 1 mM EDTA was added to the bath, the percentage of successful seals in the GΩ range was 1–2%, and with 10 mM EDTA we never observed a tight seal formation. The use of high concentrations of divalent cations, however, created a problem. More than 50% of the attempts to excise the membrane patch after formation of a GΩ seal resulted in formation of a membrane vesicle on the pipette tip. Attempts to transform the vesicle into an inside-out patch by the routine procedure of air exposure (Hamill et al., 1981) did not succeed. The swollen thylakoids ("blebs") inflated in a hypotonic "15 KCl" solution could in principle be used immediately for patch-clamp recordings as described previously (Schönknecht et al., 1988). However, the percentage of successful attempts to form GΩ seals dramatically decreased when the blebs were kept more than 15 min in this solution. To improve the formation of high resistance seals, the solution in the chamber was again replaced by the high salt "100 KCl" solution (*see* Materials and Methods for ion composition). This procedure increased the percentage of successful seals in the GΩ range from 21% to 42% (n = 100, 13 different preparations).

The analysis of single channel currents under an ion gradient across the patch had the advantage that channel selectivity could be quickly evaluated. This was particularly useful for preparations with a rapid decay of channel activity and/or containing different channel types. Besides the anion channel described here, we frequently observed two further voltage-dependent ion channels of high (several hundreds pS) conductance. Approximately one half of successful patches displayed no channel activity. Although, only a few percent of the initially formed GΩ seals resulted in successful (stable and long-lasting) recordings of single channel currents, we were able to characterize the properties of the most prominent ion channel of the thylakoid membrane in some detail. This channel was detected in approximately 25% of all successful patches and was easily identified by its high selectivity to anions.

Selectivity and Conductance of the Thylakoid Anion Channel

Figure 1 shows typical current recordings from an excised thylakoid membrane patch of *Nitellopsis obtusa,* with the intrathylakoid side facing the bath. When the concentration of KCl in the bath was changed from 15 mM (symmetrical conditions) to 100 and to 200 mM, positive currents were recorded at 0 mV, reflecting the influx of Cl^- ions from the intrathylakoid side into the

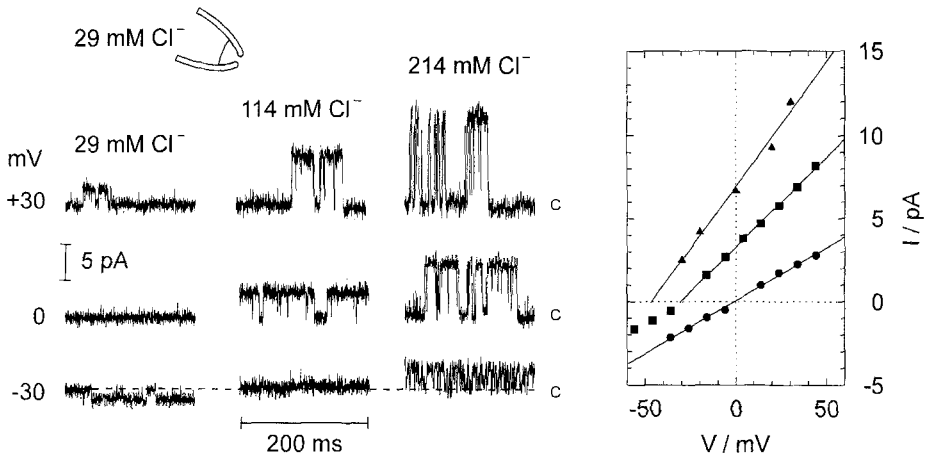

Fig. 1. Selectivity of the ion channel in the thylakoid membrane of *Nitellopsis obtusa*. Single channel traces (left) were measured in the inside-out configuration with the stromal side of the thylakoid membrane facing the solution inside the patch pipette. Given voltages refer to the stromal side of the membrane and thus positive currents correspond to a cation efflux from or an anion influx into the pipette. Original records were filtered at 2 kHz and sampled at 5 kHz. The pipette solution contained (in mM; 15 KCl, 5 $MgCl_2$, 2 $CaCl_2$, 1 EDTA, 10 HEPES-KOH, pH 7.5 (29 mM Cl^-). The bath solution was either identical (29 mM Cl^-) or with higher KCl concentrations (100 mM KCl → 114 mM Cl^-, 200 mM KCl → 214 mM Cl^-). The closed state of the ion channel is indicated by C, and for −30 mV a broken line was added to identify the closed state. Open channel currents measured at different KCl concentrations in the bath (● 15 mM, ■ 100 mM, ▲ 200 mM) were plotted against voltage (right). Single channel conductance and reversal potentials were estimated by linear regression analysis (continuous lines), ● $V(I = 0) = -1.1 \pm 0.6$ mV, $G = 64 \pm 1$ pS, ■ $V(I = 0) = -30.6 \pm 1.0$ mV, $G = 108 \pm 2$ pS, ▲ $V(I = 0) = -46.3 \pm 4.5$ mV, $G = 149 \pm 10$ pS.

pipette. The corresponding current-voltage relations are presented in Fig. 1 (right). The reversal potentials for single channel currents at asymmetrical ion conditions approached, within the accuracy of the measurements, the Nernst potentials for Cl^- (−32 and −47 mV based on ion activities calculated from the given ion gradients). This implied a high Cl^- over K^+ selectivity of the channel. The conductance of the channel in symmetrical 29 mM Cl^- was 66 ± 5 pS (n = 4), while with 114 and 214 mM Cl^- in the bath the conductance and the reversal potential (in brackets) were 102 ± 7 pS (−32.5 ± 1.1 mV; n = 10) and 146 ± 7 pS (−49.0 ± 1.0 mV; n = 3), respectively.

Voltage-dependence of the Anion Channel

The three current traces in Fig. 2 reflect the voltage-dependence of anion channel activity in an inside-out patch containing two channel copies. The recordings were made under a 29/114 Cl^- gradient across the patch to illustrate that the highest channel activity was observed at 0 mV. The steady-state kinetics of the channel at either positive or negative potentials displayed long silent periods between the bursts of activity, which were the longer the larger potentials were applied. By summing up all sample points with a certain current amplitude all-points amplitude histograms were constructed from single channel traces. These all-points histograms were fitted by a sum of Gaussian functions (Fig. 2, right). The probability to find the system at the levels C ($P(C)$), O1 ($P(O1)$) or O2 ($P(O2)$) corresponding to no, 1 or 2 channels opened was calculated from the proportion of the areas under the single Gaussians. To present the voltage-dependence of the channel quantitatively we selected patches, displaying stable single channel activity for some ten minutes (n = 4 out of 17). Interestingly, such patches always contained a functional doublet of anion channels. All-points amplitude histograms were constructed from 10 to 80 sec stretches of steady-state activity of the channels at different potentials, and the probability for the different levels ($P(C)$, $P(O1)$, $P(O2)$) was calculated by fitting a sum of Gaussian functions to the histograms. The open probability of an individual channel ($P_{O,\Sigma}$) was calculated as:

$$P_{O,\Sigma} = \frac{P(O1)}{2} + P(O2). \quad (1)$$

In Fig. 3 the open probability was plotted as a function of membrane voltage. The position of open probability maximum showed some variation from sample to sample, being in the range of 0 to +20 mV. The average of four samples is presented in Fig. 3. The observed bell-shaped voltage-dependence could formally be explained by two gating processes, one governed by positive and one by negative shift of membrane voltage, according to the following three state diagram:

$$C_1 \leftrightarrow O \leftrightarrow C_2 \quad (2)$$

where C_1 and C_2 are closed states occupied at negative

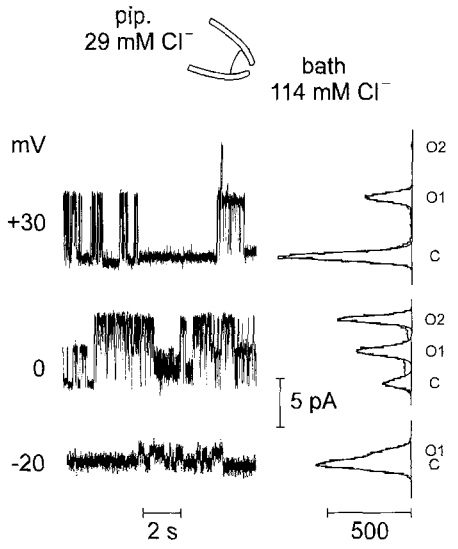

Fig. 2. Voltage-dependence of the anion channel. The single channel traces represent steady state channel activity, during 10 sec time periods when the voltage was held at +30, 0 or −20 mV. On the right the corresponding all-points amplitude histograms are shown, indicating the number of sample points with a certain current amplitude (the bar at the lower right corresponds to 500 sample points). The all-points histograms were fitted by a sum of Gaussian distributions. Current levels are identified as C for the closed state and O1 or O2 for one or two open channels. Original records were filtered and sampled at 500 Hz. Pipette and bath solutions as given in Fig. 1 (pipette 20 mM Cl^-, bath 114 mM Cl^-).

and positive potentials, respectively and O is the open state. We assumed that the equilibrium between each closed state (C_i) and the open state (O) could be described by a Boltzmann distribution in the form

$$\frac{C_i}{O} = \exp \frac{z_i F \cdot (V - V_i)}{RT} \tag{3}$$

where V is the voltage, z_i is the effective valence of the gating charge, V_i is the voltage at which the probability to find the channel in the state C_i or O is equal. F, R, and T have the usual meaning. For the three state diagram given by Eq. 2 (i = 1,2) the open probability ($P_{O,\Sigma}$) as a function of voltage (V) could be expressed as

$$P_{O,\Sigma} = 1 \Big/ \left(1 + exp \frac{z_1 F \cdot (V - V_1)}{RT} + exp \frac{z_2 F \cdot (V - V_2)}{RT} \right). \tag{4}$$

A nonlinear regression analysis yielded the following parameter values, z_1 = −2.2, V_1 = −3.4 mV, z_2 = 1.9, V_2 = 12.1 mV. As can be seen in Fig. 3 (bottom), the position of the open probability maximum was changed insignificantly when the ionic conditions were switched from asymmetrical 29 Cl^-/114 mM Cl^- to symmetrical 29 mM Cl^-. However, the open probability in the latter case

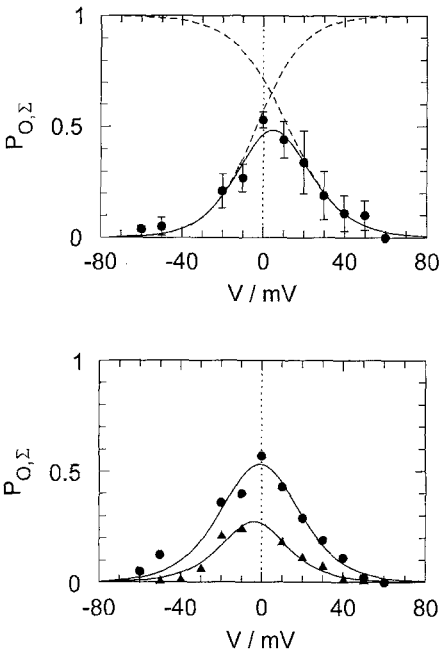

Fig. 3. Open probability ($P_{O,\Sigma}$) of the voltage-dependent anion channel as a function of voltage. All-points amplitude histograms from single channel recordings lasting between 10 and 80 sec were fitted by a sum of Gaussian distributions as depicted in Fig. 2 to calculate the open probability. Top, data from four different patches (pipette 29 mM Cl^-, bath 114 mM Cl^-) were averaged and displayed as mean ± SD (error bars). The data points were fitted by Eq. 4 resulting in z_1 = −2.2 ± 0.6, V_1 = −3.4 ± 3.6 mV, z_2 = 1.9 ± 0.4 and V_2 = 12.1 ± 3.7 mV (continuous line). The broken lines indicate the corresponding Boltzmann functions according to Eq. 3 which describe the voltage-dependent equilibrium $C_1 \leftrightarrow O$ and $O \leftrightarrow C_2$, respectively (*see* Eq. 2). Bottom, data from a single patch without (▲ bath and pipette 29 mM Cl^-) and with ion gradient (● pipette 29 mM Cl^-, bath 114 mM Cl^-). The data were fitted by Eq. 4 with z_1 and z_2 fixed to −2.0 and 2.0, respectively (continuous lines), ▲ V_1 = −0.3 ± 1.6 mV, V_2 = −7.4 ± 1.8 mV, ● V_1 = −11.4 ± 1.9 mV, V_2 = 9.5 ± 1.6 mV.

was substantially decreased over the whole voltage range (n = 2). This effect was fully reversible, and the open probability increased again when the high salt solution was returned to the bath (*not shown*). It should be noted that while the steady state activity of the channel at large (>30 mV) potentials of either sign was very low, direct transitions from positive to negative potentials and *vice versa* were always accompanied by transient channel openings (Fig. 4). This can be understood on the basis of the kinetic scheme given in Eq. 2. According to this scheme a transition from the closed state occupied at large negative potentials to that occupied at positive potentials and *vice versa* takes place through the open state.

Fast Gating of the Anion Channel

The examples of single channel traces presented in Figs. 1 and 2 provide evidence for a bursting behavior of the

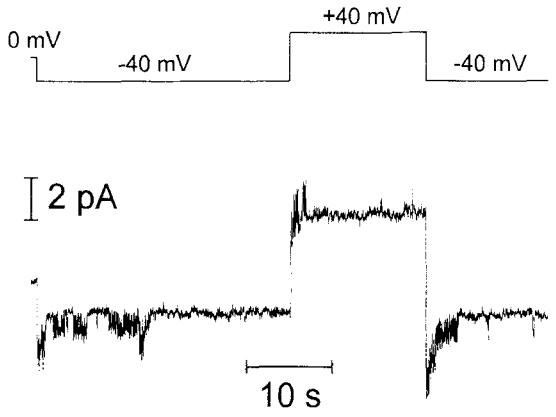

Fig. 4. Transient activation of the voltage-dependent anion channel by voltage jumps. From a holding potential (top) of 0 mV the potential was stepped to −40 then to +40 and again back to −40 mV. Each voltage jump resulted in a rapid increase of single-channel activity which decayed within a few seconds. Original records were filtered and sampled at 50 Hz. Symmetrical pipette and bath solutions (29 mM Cl^-) as given in Fig. 1.

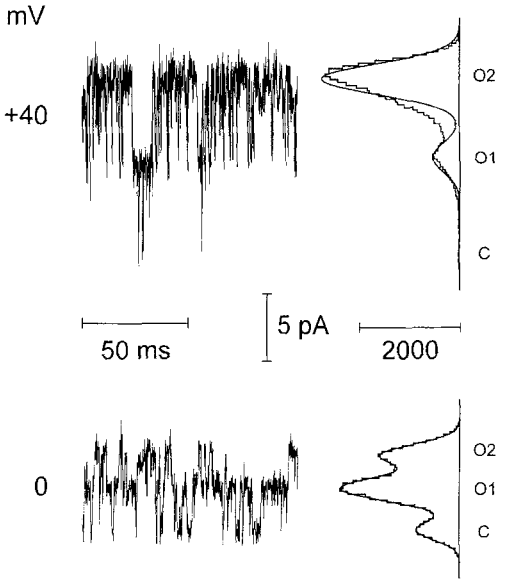

Fig. 5. Voltage dependence of the fast gating in the anion channel. Short segments of single channel traces were selected which did not contain long channel closures. On the right all-points amplitude histograms fitted by Gaussian distributions are shown. About 100 segments of 50 msec duration at each given voltage were used to construct the all-points histograms (the bar at the right corresponds to 2000 sample points). Current levels are identified as *C* for the closed state and *O1* or *O2* for one or two open channels. Original records were filtered at 3 kHz and sampled at 10 kHz. Pipette and bath solution as given in Fig. 1 (pipette 29 mM Cl^-, bath 114 mM Cl^-).

channel. There are at least two dwell-time components for the closed state, one within the millisecond time range (*intraburst* closures) and another one, slower by at least one order of magnitude, up to the seconds time range (*interburst* intervals). A proper analysis of the longer *interburst* closed dwell-times required relatively long (several minutes) recordings at each potential. However, this was impossible because of the low stability of thylakoid patches at large (>30 mV) potentials. Therefore, we restricted the kinetic analysis to *intraburst* single channel transitions taking place at a fast time scale (t < 50 msec).

When the membrane potential is switched to a new value, and as soon as a channel opening is observed, the equilibration of the open state with neighbouring closed state(s), available in the milliseconds time scale, occurs also in milliseconds. Thus, the transient channel activity at large membrane potentials, observed for only a few seconds after a voltage step (e.g., Fig. 4), can be analyzed on the milliseconds time scale. These short intervals contained sufficient information regarding the distribution of the channel dwell-times on the milliseconds time scale. Practically, the voltage range up to 50 mV could be examined in this way here.

As mentioned above, patches with stable channel activity usually displayed a doublet of anion channels. This also holds for current transients at larger membrane voltages (>30 mV; Fig. 5 and 8). From digitized single channel recordings only 50 msec segments *without* long (>20 msec) channel closures were used to construct all-points amplitude histograms, to analyze the fast gating only. These were fitted by a sum of three Gaussian functions corresponding to the closed level (C), and one (*O1*) or two channels opened (*O2*) (Fig. 5) and the probability for each level ($P(C)$, $P(O1)$, $P(O2)$) was calculated. From these probabilities the open probability for the channel within a burst ($P_{O,B}$) was estimated as in Eq. 1 (*see* Table). As one can see from a direct comparison of Fig. 5 with Fig. 2 the open probability within a burst ($P_{O,B}$, Fig. 5) was completely different from the total open probability ($P_{O,\Sigma}$, Fig. 2), as the latter includes the long closed times between bursts. To test whether within a burst gating of the two channels was independent, the theoretical probability for the different levels ($P^*(C)$, $P^*(O1)$, $P^*(O2)$) was recalculated from the open probability ($P_{O,B}$) assuming a binomial distribution:

$$P^*(C) = (1 - P_{O,B})^2, \quad P^*(O1) = 2 \cdot P_{O,B} \cdot (1 - P_{O,B}), \quad P^*(O2) = P_{O,B}^2 \tag{5}$$

No significant deviation from a binomial distribution was found (χ^2 test, Table) indicating that the gating of the two channels was independent within a burst.

The kinetic behavior of this double-channel system was characterized at different voltages. We analyzed dwell-times distributions for the level with both channels closed (*C*) and for the level with both channels open (*O2*). The dwell-times histograms shown in Fig. 6 (top) were constructed from single-channel traces of 20-sec duration on the basis of event lists (idealized single chan-

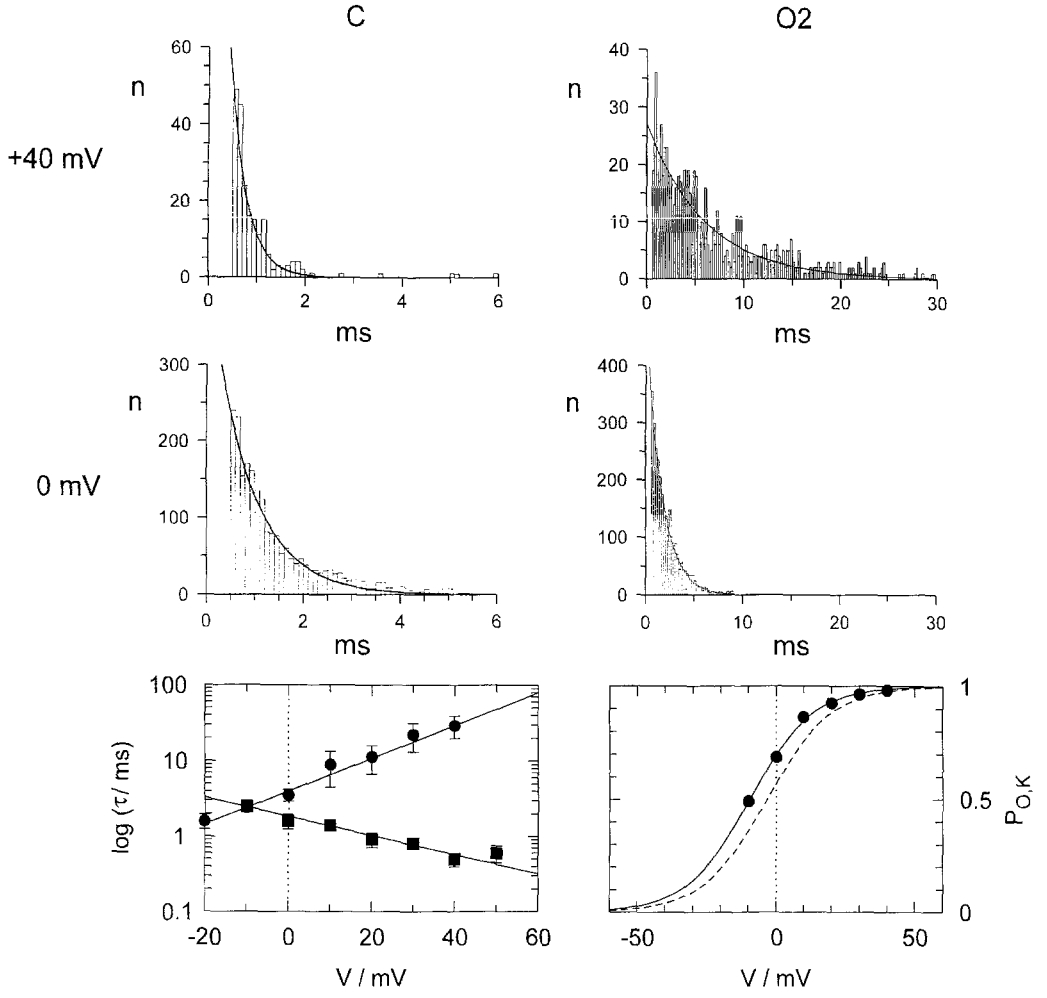

Fig. 6. Voltage-dependence of the fast kinetics of the anion channel. Top, distribution of dwell-times at level *C* (no channel open) and level *O2* (both channels open) for two voltages. Dwell-times histograms were constructed from 20 sec recordings of single channel activity filtered at 3 kHz and sampled at 10 kHz with a bin width of 0.2 msec (n gives the number of events with a certain dwell time). The solid lines indicate monoexponential fits of the dwell-times histograms (+40 mV, *C*, $\tau = 0.34 \pm 0.13$ msec, *O2*, $\tau = 6.03 \pm 0.01$ msec, 0 mV, *C*, $\tau = 0.85 \pm 0.04$ msec, *O2*, $\tau = 1.63 \pm 0.02$). Bottom left, semilogarithmic plot of the voltage-dependence of the mean open (●) and mean closed time (■) for the individual anion channel. Data from three different patches were averaged and shown as mean ± SD (error bars). Data were fitted assuming an exponential dependence of the mean open and mean closed time from the voltage according to Eq. 7 (● $\tau_0 = 3.89 \pm 0.13$ msec, $\varphi = 20.0 \pm 1.2$ mV, ■ $\tau_0 = 1.82 \pm 0.08$ msec, $\varphi = -35.7 \pm 3.8$ mV). Bottom right, voltage-dependence of intraburst open probability ($P_{O,K}$) as calculated by Eq. 8 from the mean open and mean closed times presented in the left. The continuous line indicates a Boltzmann distribution fitted to the data according to Eq. 3 ($z_0 = -2.26 \pm 0.09$, $V_0 = -9.6 \pm 0.4$ mV). The dashed line indicates the Boltzmann function which describes the voltage dependent equilibrium $C_1 \leftrightarrow O$ according to Eq. 2 ($z_1 = -2.2 \pm 0.6$, $V_1 = -3.4 \pm 3.6$ mV, *cf.* Fig. 3). Pipette and bath solution as given in Fig. 1 (pipette 29 mM Cl^-, bath 114 mM Cl^-).

nel traces). The different number of events (n) at +40 and 0 mV reflects the lower channel activity at +40 mV (*see* Fig. 3). All dwell-times histograms could be satisfactory described by a monoexponential time-dependence

$$n = n_o \cdot e^{-t/\tau}. \quad (6)$$

This indicates that the two channels are not only independent but also kinetically identical, and that closed and open times distributions within the examined time frame are monoexponential. Compared to the many fast transitions within bursts only very few longer closed times between bursts were added up. Therefore our kinetic analysis reflects the channel behavior within bursts. In the case when both channels were closed (at current level C), the mean time to observe the opening of one of the two channels will be two times shorter as compared to the mean closed time for the individual channel. The same holds for the dwell-times at current level *O2*. Therefore, mean closed and open times for individual channels could be calculated by multiplying the observed dwell-times (Fig. 6, top) by a factor of two. The voltage dependence of the mean closed and mean open

Table. Test for independent gating of two anion channels and comparison of open probabilities calculated by two different methods

V/mV	Level	P	$P_{O,B}$	P^*	χ^2	τ_{cl}/msec	τ_{op}/msec	$P_{O,K}$
	C	0.003		0.003				
+50	*O1*	0.117	0.94	0.113	0.9999	0.70	12.20	0.95
	O2	0.881		0.884				
	C	0.005		0.006				
+40	*O1*	0.131	0.93	0.139	0.9997	0.68	12.06	0.95
	O2	0.864		0.856				
	C	0.011		0.014				
+30	*O1*	0.226	0.88	0.211	0.9991	0.66	6.40	0.91
	O2	0.764		0.774				
	C	0.043		0.048				
+20	*O1*	0.359	0.78	0.343	0.9932	0.92	4.52	0.83
	O2	0.598		0.608				
	C	0.078		0.090				
+10	*O1*	0.446	0.70	0.420	0.9982	1.30	3.92	0.75
	O2	0.476		0.490				
	C	0.140		0.152				
0	*O1*	0.500	0.61	0.476	0.9987	1.70	3.26	0.66
	O2	0.360		0.372				
	C	0.283		0.281				
−10	*O1*	0.500	0.47	0.498	0.9999	2.44	2.60	0.52
	O2	0.217		0.221				
	C	0.331		0.372				
−20	*O1*	0.519	0.39	0.476	0.9958	2.80	1.88	0.40
	O2	0.149		0.152				

Current fluctuations were recorded in a single patch at membrane potentials from +50 to −20 mV (first column). Each all-points amplitude histogram was constructed from hundred 50 msec segments without long (>20 msec) closures and fitted by a sum of Gaussian distributions (*see* Fig. 2). For the three levels *C*, *O1* and *O2* ("Level") the probability for each level (P) was calculated from the proportion of the Gaussian peaks. From these values the open probability ($P_{O,B}$) was calculated according to Eq. 1. Assuming a binomial distribution for independently gating channels $P_{O,B}$ was recalculated into theoretical probabilities (P^*) for the levels *C*, *O1* and *O2* according to Eq. 5. A chi-square test (χ^2) revealed that the experimental data did not deviate from the theoretical prediction. The gating of the two channels was independent from each other within a burst. From the same single channel traces, dwell-times distributions were constructed for 20 sec recordings for the levels *C* and *O2* (*see* Fig. 6). Monoexponential fits of the dwell-times histograms were used to calculate the mean closed and mean open times of the individual channel (τ_{cl} and τ_{op}). From the mean closed and mean open times the open probability ($P_{O,K}$) was calculated according to Eq. 8.

times for the individual channel were plotted in Fig. 6 (bottom, left). The data shown are averages from three patches and for each single τ value a continuous 20-sec recording was analyzed as just described. The mean closed time (τ_{cl}) and the mean open time (τ_{op}) were exponentially dependent on the applied voltage

$$\tau = \tau_0 \cdot e^{V/\varphi} \tag{7}$$

where τ_0 is the mean closed/open time at 0 mV, and φ gives the steepness of the voltage dependence. The mean time spent in the opened state increased e-fold by a +20 mV shift of the membrane voltage, while an e-fold decrease of the mean closed time required a +36 mV shift.

To test the consistency of the different approaches, the intraburst open probability based on this kinetic analysis ($P_{O,K}$) was calculated as:

$$P_{O,K} = \frac{\tau_{op}}{\tau_{cl} + \tau_{op}} \tag{8}$$

and compared with $P_{O,B}$ computed according to Eq. 1 after fitting Gaussian functions to the corresponding all-points amplitude histograms obtained from segments without longer (>20 msec) channel closures. In the Table the open probabilities at different potentials as determined in this way ($P_{O,B}$) were compared with those calculated from dwell-times using Eq. 8 ($P_{O,K}$). The agreement between the two independent analytical approaches to estimate the open probability within bursts provides evidence for the correct treatment of single channel kinetics in the millisecond time domain. Slightly larger values for $P_{O,K}$ compared to $P_{O,B}$ (Table) are likely due to the presence of a small number of longer closures included. These provide no significant effect to the dwell-times distributions, where events of different duration have the same statistical weight. But longer closures significantly contribute to the distribution of the current levels in all-points amplitude histograms, where the number of counts is proportional to the time spent at given level. For this reason, the values calculated by Eq. 8 ($P_{O,K}$) provide more exact estimates for the intraburst

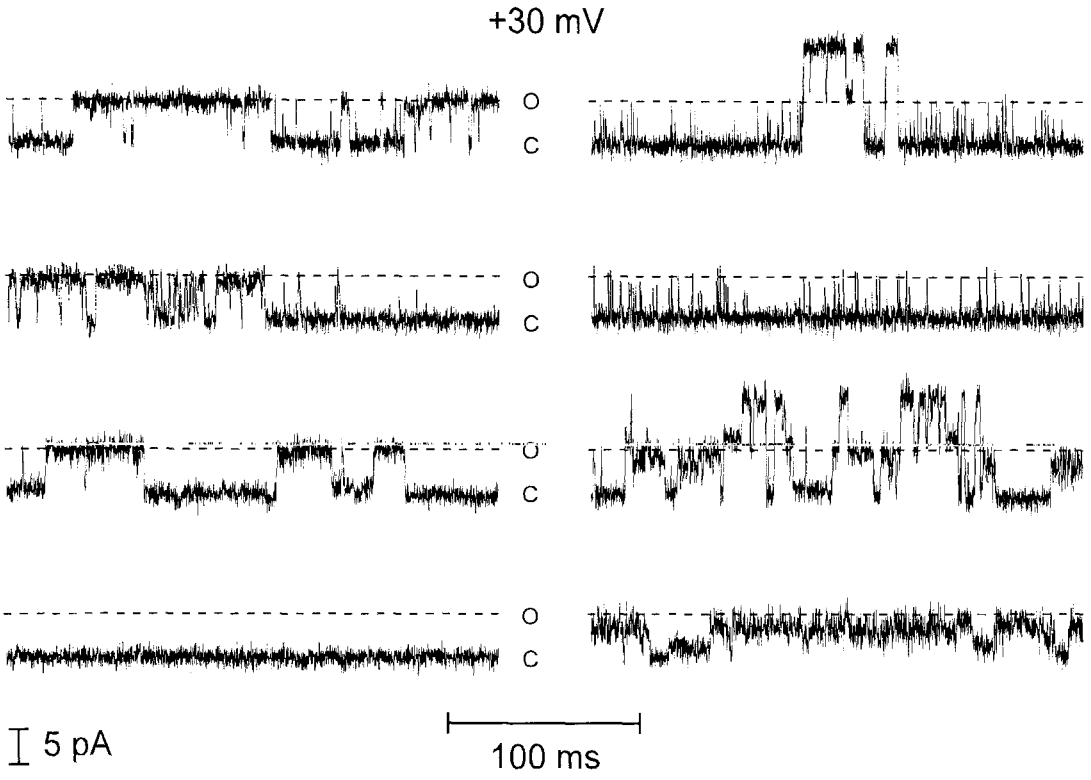

Fig. 7. Complex kinetics of the voltage-dependent anion channel. The voltage was stepped to +30 mV and 1 sec of continuous recording is shown by the four consecutive single channel traces on the left. Within 1 min this procedure was repeated with the same patch resulting in the four (continuous) single channel traces on the right. The continuous line indicates the open state (*O*) of a single channel. Original records were filtered at 3 kHz and sampled at 10 kHz. Pipette and bath solution as given in Fig. 1 (pipette 29 mM Cl^-, bath 114 mM Cl^-).

open probability. We calculated the open probability ($P_{O,K}$) using Eq. 8 from mean closed and open time values as given in Fig. 6 (bottom left), and plotted them as a function of membrane voltage (Fig. 6, bottom right). The resulting data points could be described by a two-state Boltzmann distribution (Eq. 3) with an effective gating charge $z_0 = -2.26$ and a midpoint potential of $V_0 = -9.6$ mV. The voltage-dependence of the intraburst open probability ($P_{O,K}$) and the voltage-dependence of the total open probability ($P_{O,\Sigma}$) (Fig. 3) at negative potentials could be described by similar Boltzmann distributions (Fig. 6, bottom right, continuous line and broken line). However, the voltage-dependence of the total open probability ($P_{O,\Sigma}$) was shifted by +6 mV as compared to the voltage-dependence of the intraburst open probability ($P_{O,K}$). Apparently, long closures between bursts of activity at negative potentials (Fig. 2) decreased the total open probability ($P_{O,\Sigma}$) as compared to the intraburst open probability ($P_{O,K}$). As the parameter z describing the steepness of voltage-dependence of $P_{O,\Sigma}$ and $P_{O,K}$ was approximately the same (≈–2.2) the simplest way for a more appropriate description of channel gating at negative potentials was to include an additional closed state by splitting of C_1 of Eq. 2 into two states, $C_{1,1}$ and $C_{1,0}$:

$$C_{1,1} \leftrightarrow C_{1,0} \underset{\tau_{op}}{\overset{\tau_{cl}}{\leftrightarrows}} O \leftrightarrow C_2 \qquad (9)$$

with a voltage-independent ratio $C_{1,1}/C_{1,0} = 0.7$ to account for the observed 6-mV shift (Fig. 6, bottom right).

Double-amplitude Transitions, Subconductance States and Flickers

The kinetic behavior of the channel as described above was, however, a simplified view. More kinetic peculiarities have been revealed. Figure 7 shows two sets of traces of continuous channel activity at +30 mV of 1 sec duration each, measured within 1 min (first left then right four traces) with the same sample, containing two anion channel copies. The left panel demonstrates the "typical" activity of a single channel, which closed completely at the end of the record. The right panel, however, demonstrates some types of kinetic peculiarities we observed. First, simultaneous openings and closures of two channels were observed (first trace from the top). The channel displayed very short and only partly resolved openings ("flickers", second trace). Kinetic analysis performed for this mode of activity revealed

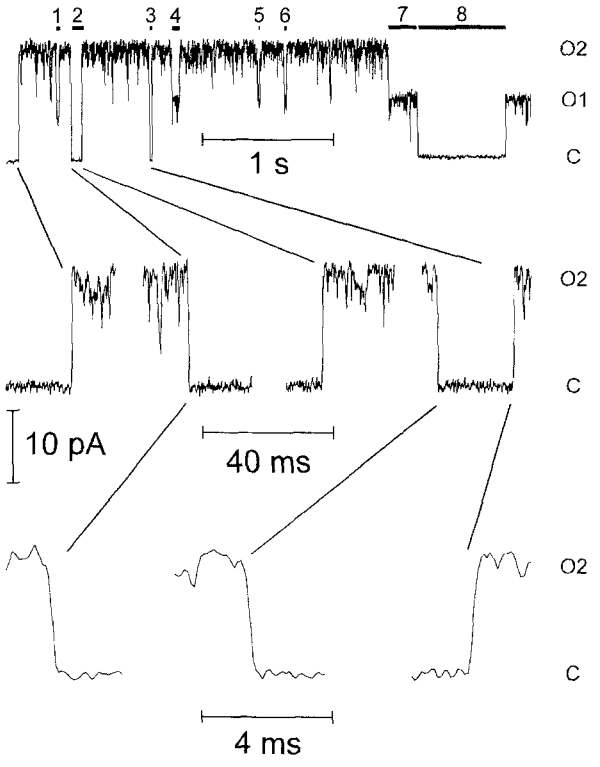

Fig. 8. Simultaneous openings and closures of two anion channels. Example of current transitions among three different current levels recorded at +50 mV. Channel closures lasting longer than 20 msec are indicated by black bars above the trace consecutively numbered. Current levels are identified as *C* for the closed state and *O1* and *O2* for one or two open channels. Some direct transitions where two channels opened or closed simultaneously are displayed at expanded time scales. The straight lines connect identical transitions. Original records were filtered at 3 kHz and sampled at 10 kHz, the upper trace was additionally digital filtered at 200 Hz. Pipette and bath solution as given in Fig. 1 (pipette 29 mM Cl^-, bath 114 mM Cl^-).

mean open times in the range of 0.3–1.0 msec (voltage range from −20 to +30 mV) as compared to 1.5 to 20 msec in the "normal" mode (*see* Fig. 6). Further, transitions to lower subconductance states were observed (two bottom traces, see also Fig. 9).

Direct transitions of double amplitude were common for most of the patches containing several copies of anion channels (5 out of 7). A more detailed example of this behavior is presented in Fig. 8. While closed-open transitions of two channels in the millisecond time scale could be explained by binomial statistics (*see* above), which means they were kinetically independent, the transitions to and from the long closed states often occurred in concert. Let us now consider only closed dwell-times longer than 20 msec and intervals between them, the time domain at which the two channels seem to open/close together. At +50 mV (Fig. 8), the 20 msec cutoff is sufficient to separate fast channel closures within a burst, which have a characteristic time of 0.5–0.7 msec (Fig. 6) from slower components of the closed dwell-times distribution. Ignoring fast channel gating the trace shown in Fig. 8 (top) can be divided in 8 long closures and 7 intervals between them, with a mean duration of 140 ± 80 msec and 345 ± 105 msec, respectively. Among these transitions three occurred from the baseline (C, both channels closed) directly to the top level (O2, both channels open) and two in opposite direction, apparently bypassing the intermediate state (O1). To prove this the 5 direct transitions are displayed at expanded time scale (Fig. 8, middle) and further 3 of them at a more expanded time scale (Fig. 8, bottom). Analysis of the digitized trace showed that all these 5 direct transitions of double amplitude contained only 3 to 5 samples of 0.1 msec each, i.e., occurred within 0.2–0.4 msec. Assuming an independent behavior of two monomeric channels and taking the above values for closed and open intervals, one calculates the probability of two channels to close (open) within 0.3 msec interval as 0.3/345 (0.3/140) or 0.00087 (0.0021). The observed probability of closure (opening) of two channels in concert for this current record was more than 100 times higher, 2/7 = 0.286 (3/8 = 0.375). Simultaneous transitions of two channels between closed and open state without any detectable transition to the intermediate state corresponding to one open channel were observed frequently, irrespective to the applied potential. Therefore, there exists a common slow gating mechanism for the two channel aggregate, while the fast millisecond transitions of the monomeric channels appeared to be independent and, hence, should be produced by local gates.

Although the current through the single monomeric channel usually fluctuated between zero and fully open state with a conductance of 100–110 pS in 29/114 mM Cl^- gradient (Fig. 1), the contribution of lower subconductance states could not be completely neglected, and the substates were observed in most of the patches examined. The most frequently observed substates had a conductance of approximately 75%, 50%, and 25% of that in the fully open state (Fig. 9). The distribution of dwell-times at substates could differ from that in the fully open state (*not shown*), and the transition to a substate was often accompanied by an increase in current noise as shown in Fig. 7 (right, bottom trace). Despite these differences in conductance and kinetic behavior, the selectivity of substates was the same as for the fully open state (Fig. 9).

Discussion

The Anion Channel as an Obligatory Component of Thylakoid Membrane

In this study we demonstrated the presence of high selective voltage-dependent anion channel in the thylakoid

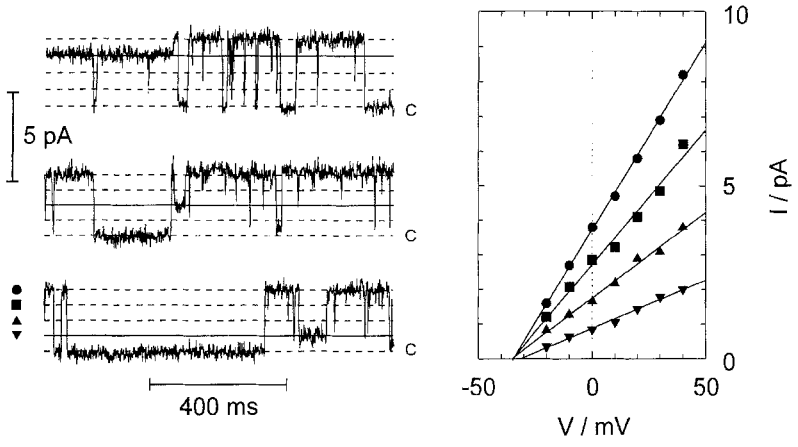

Fig. 9. Subconductance states of the voltage-dependent anion channel in the thylakoid membrane of *N. obtusa*. Single channel traces (left) were measured at 0 mV (inside-out). Original records were filtered at 0.5 kHz and sampled at 1 kHz. The closed state of the ion channel is indicated by *C*, broken lines indicate current levels with amplitudes of n-times (n = 0 . . . 4) 25% of the main conductance level. Examples for the conductance substates (indicated by solid lines) with amplitudes of approximately 75% (■), 50% (▲), and 25% (▼) of the main level are given. Single channel currents for the main conductance (●) and three subconductance states (■ ▲ ▼) were plotted against voltage (right). The different conductance levels and the reversal potential were calculated from linear regression analysis (continuous lines), ● $V(I = 0) = -34.6 \pm 1.0$ mV, $G = 108 \pm 2$ pS, ■ $V(I = 0) = -34.6 \pm 3.5$ mV, $G = 78 \pm 5$ pS, ▲ $V(I = 0) = -35.0 \pm 2.4$ mV, $G = 50 \pm 2$ pS, ▼ $V(I = 0) = -31.4 \pm 2.2$ mV, $G = 28 \pm 1$ pS. Pipette and bath solution as given in Fig. 1 (pipette 29 mM Cl^-, bath 114 mM Cl^-).

membrane of chloroplasts isolated from the green alga *Nitellopsis obtusa*. The permeability characteristics of this channel and of the one previously described in the photosynthetic membrane of the higher plant *Peperomia metallica* (Schönknecht et al., 1988), were almost identical. Under asymmetrical ion conditions both channels displayed a reversal potential corresponding to the Nernst potential for Cl^-. Furthermore, comparison of their single-channel conductance (G) as a function of Cl^- concentration revealed the same pattern, with the experimental errors overlapping (Fig. 10). The dependence for the *P. metallica* anion channel was previously explained by a Michaelis-Menten model with one binding site, $K_m = 40$ mM; and $G_{max} = 150$ pS (as shown by the continuous line in Fig. 10). It appears, however, as though this model might not sufficiently describe the datapoints at high Cl^- concentrations. Thus, a more complex formalism, with an additional low affinity binding site for Cl^- might be more appropriate. The anion channels in the thylakoid membrane of *P. metallica* and *N. obtusa* appear to have a similar set of conductance substates of approximately 1/4, 1/2, and 3/4 of the conductance in the fully open state (*cf.* Figs 7 and 9 of this study and Fig. 2 by Schönknecht et al., 1988). These two channels have a bell-shaped voltage-dependence, with a decrease of steady-state single channel activity at both positive and negative membrane potentials. However, the position of maximum open probability differed between these two species. For *N. obtusa* the maximum channel activity was observed close to 0 mV, while Schönknecht et al. (1988) reported the maximum activity at around –40 mV (stromal side negative) in *P. metallica*.

Results obtained with spinach thylakoids (Pottosin & Schönknecht, 1995) show that the high selective anion channel with a conductance of 75 to 110 pS in 100 mM KCl exists in this species as well. In spinach thylakoids an additional low-conductance cation channel was characterized (I.I. Pottosin & G. Schönknecht, *in preparation*) which was never observed in *N. obtusa* or *P. metallica* thylakoids. So far, the anion channel, now proved to be present in the thylakoid membrane of different plant species, escaped detection in reconstitution studies

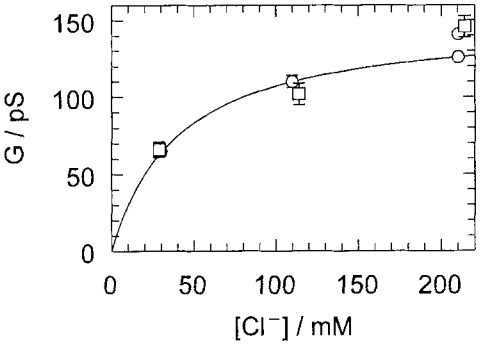

Fig. 10. Conductance (G) as a function of Cl^- concentration for single anion-selective channels in thylakoid membranes from *Peperomia metallica* and *Nitellopsis obtusa*. The single channel conductance was estimated by linear regression analysis of experimental current-voltage relationships as those presented in Fig. 1. (□) *N. obtusa*, data of this work, pipette solution contained 29 mM Cl^-, bath 29, 114 or 214 Cl^-, the complete ion composition as given in Fig. 1 (○), *P. metallica*, the data of Schönknecht and coworkers (1988), the ion composition of the media was similar, but pipette solution contained 32 mM Cl^- and bath 30, 110 or 210 mM Cl^-. Solid line was drawn assuming a Michaelis-Menten behavior of the open channel, with $K_m = 40$ mM and $G_{max} = 150$ pS.

done with spinach thylakoids (Tester & Blatt, 1989; Enz et al., 1993). We frequently observed a fast rundown of anion channel activity in excised patches. In a reconstitution system a rapid rundown may result in a complete decay of channel activity before the measurement can even be started. Another problem with the reconstitution of thylakoid membrane is that this membrane contains a high concentration of H^+-ATPase, whose damage under reconstitution conditions leads to detection of cation channels generated by the channel part (CF_0) of this enzyme (Schönknecht et al., 1989). This results in a large activity of cation channels in reconstitution studies which do not exist in the native thylakoid membrane and which hamper the analysis of other ion channels. The use of the native thylakoid membrane allowed us to characterize a prominent anion channel, not detected in reconstitution studies.

The characteristics of the thylakoid anion channel were comparable to the properties of a similar channel measured in the chloroplast envelope of *Nitellopsis obtusa* (Pottosin, 1992). The latter channel, however, seems to have larger conductance (160 pS in symmetrical 0.1 M KCl or 330 pS in 0.5/0.1 M KCl gradient). Further, while the reversal potential for the thylakoid channel under a 3.5-fold KCl gradient was –32 mV, implying an "ideal" Cl^-/K^+ selectivity, the envelope channel displayed a reversal potential of –30 mV with a 5-fold KCl gradient. The voltage-dependence was, however, apparently the same, with maximum channel activity at 0 mV, and the open probability of both channels similarly increased with an increase of the salt concentration on one side of the membrane. It can not be excluded that these channels are identical, and further comparison of their biophysical characteristics under the same ionic conditions is required to test this possibility.

Gating of the Thylakoid Anion Channel

The analysis of the anion-selective channel in *Nitellopsis obtusa* thylakoid membranes revealed two separate kinetic domains. Bursts of activity, when the single-channel current fluctuated between closed and open states in the millisecond range, were interspersed by long (up to seconds) "silent" periods. The fast-gating showed a voltage dependence in such a way that more positive membrane voltages increased the probability of the open state (Fig. 6, bottom, right; Table). On the other hand, the probability of burst appearance decrease at more positive membrane voltages because of longer closed times (Fig. 2). Since the channel is open only when both gates, the fast and the slow one, are open, the voltage-dependence of the channel as a whole displayed a bell-shaped form given by the two Boltzmann distributions (Fig. 3, top). For a better description of the resulting voltage-dependence at negative potentials an additional closed state was included (Eq. 9). The four-state model presented by Eq. 9 is a minimal scheme, with a minimal number of slow components for closed times. One closed state for positive and one for negative voltages were considered to account for the long closed times between bursts of single channel activity. To be complete, the scheme should also explain the different modes of activity as, for example, simultaneous openings or closures of two channels, the very short channel openings (Fig. 7) and the appearance of intermediate conductance states (Figs. 7 and 9). Although our scheme does not account for all these details of the channel kinetics, it nevertheless gives an accurate description of the mean open channel probability as a function of membrane voltage. And it can be used as a starting point for comparison of gating in thylakoid channels with gating models for anion channels of other origin.

One aspect, not reflected by Eq. 9 but clearly documented in Figs. 7 and 8, is the "double-barrelled-like" behavior that requires special attention. There are only few anion channels, known from animal systems which display a comparable double-barrelled-like behavior. A detailed kinetic analysis was carried out for the 9 pS channel from *Torpedo* electroplax (White & Miller, 1979; Miller, 1982) and recently for the 160 pS channel from rat liver rough endoplasmic reticulum (Morier & Sauve, 1994). "Double-barrelled" channels can be defined by the following characteristics. (i) In the millisecond time domain the behavior of the aggregate, formed by two channels of identical conductance and selectivity, follows binomial statistics. Thus the fast transitions of the two channels are independent of each other with a simple closed-open kinetics for the monomeric channel displaying a monoexponential dwell-times distribution. (ii) In the time domain of tens of milliseconds to seconds the aggregate of two channels converts between the open and long inactivated states in concert. There are direct transitions between the level with both channels closed and the level with both channels open. Besides these common characteristics, which also hold for the channel described here, the voltage-dependent gating in double-barrelled anion channels can be different. The low-conductance channel described by Miller's group (White & Miller, 1979; Miller, 1982) has a bell-shaped voltage-dependence of open probability similar to that found for the 100 pS anion channel from *N. obtusa* thylakoid membranes. The bell-shaped voltage-dependence of *Torpedo* channel was also explained as a product of two different gating processes. The fast gate, facilitating channel closure upon membrane hyperpolarization, has a voltage dependence with an equivalent gating charge $z = -1.1$ as compared to $z = -2.2$ for the *N. obtusa* channel. The slow gate, responsible for long closed times between bursts of channel activity, switched the channel to the nonconducting state at depolarization. This gating process has almost the same steepness of

voltage-dependence in *N. obtusa* and *Torpedo* ($z = 1.9$ and $z = 2.2$). The position of maximum open probability was different, however, at 0 and −50 mV for *N. obtusa* and *Torpedo* anion channels, respectively. The anion channel from rat liver rough endoplasmic reticulum has a single channel conductance comparable to *N. obtusa*, but displayed a different voltage gating. Both the probability of burst formation and the intraburst open probability for this channel increased at more positive membrane potentials (referring to the cytoplasmic side). Although the fast gating and the voltage-dependence of both mean closed and mean open times in endoplasmic reticulum channel were similar to that measured for the thylakoid channel in the present work, the former channel apparently lacks the slow gate which caused the inactivation of the *N. obtusa* channel at positive membrane potentials.

A slightly anion-selective ($P_{Cl}/P_K = 4.5$) voltage-dependent 107 pS channel, also called mCs (mitochondrial Centum pico-Siemens), was described in the inner mitochondrial membrane (Sorgato, Keller & Stühmer, 1987; Sorgato & Moran, 1993). Again, the fast gating of this channel was similar to that found in the thylakoid anion channel. The data of different authors, although showing some variation, provide evidence that the mean closed time for the mCs channel is relative weakly voltage-dependent, being in the range of 0.5–2.0 msec at positive potentials, while the mean open time value varies between 7 and 52 msec in the voltage range of +40 to +60 mV, and decreased at least sixfold when the membrane voltage was stepped to negative values (Sorgato & Moran, 1993; *cf.* Fig. 6 bottom-left, this study). However, the mitochondrial channel also lacks the slow gating process at positive potentials, so the macroscopic current through the whole mitoplast membrane showed an outward rectification (Sorgato et al., 1987). It should be noted that a bell-shaped voltage-dependence with a maximum at around 0 mV as described here is not a unique characteristic of the thylakoid anion channel since it was found for many large conductance anion channels in the plasma membrane of different animal cells (Franciolini & Adams, 1994) as well as for the mitochondrial outer membrane anion channel, VDAC (Colombini, 1989).

The appearance of lower conductance substates is also a common feature of large conductance anion channels. However, the mechanisms of their generation are probably different in different channels. As an example, in VDAC the selectivity is changed from slightly anionic to cationic upon channel transition from the fully open state to the state with a conductance of about 40% of the maximum (Colombini, 1989). Given both the different selectivity of conductance states in VDAC and that the main conductance could not be described by a sum of subconductance levels, this implies a conformational change within a single pore as a mechanism of generation of different conductance states. This mechanism is unlikely for the *N. obtusa* thylakoid channel, as the selectivity of lower conductance states for this channel was the same as of the fully open state, and the conductance could be divided in levels of approximately n-times 25% of the main conductance (Fig. 9). The latter observation is in line with another class of models, which consider a large conductance channel as a homo-oligomer of smaller conductance channels. For the large conductance anion channel from the plasma membrane of molluscan neurone up to 16 equally-sized subconductance levels are reported. Moreover, during the degradation of the channel activity in isolated patches the smaller channels started to behave as independent entities (Geletyuk & Kazachenko, 1985). Although this model seems to be a plausible explanation of the behavior of thylakoid anion channels, we never observed patterns with four independently gating identical channels, each having a conductance of 25% of that in the main state. Further, the apparent subconductance states might be a product of very fast channel flickering, measured at limiting time resolution (Draber & Hansen, 1994), as found, for instance, for voltage-dependent fast chloride channels when they switch to so called "buzz" mode (Blatz & Magleby, 1986). We observed substates often in parallel with fast channel flickering as shown in Fig. 7. In some cases, the current noise increased when the channel switched from the main to an intermediate conductance state (Fig. 7, bottom, right) which might be an evidence for only partly resolved fast channel flickering.

Possible Physiological Role of the Voltage-dependent Anion Channel in Thylakoid Membrane

The uptake of anions in thylakoids as well as concomitant efflux of K^+ and Mg^{2+} in the light are thought to be involved in the maintenance of electroneutrality during massive light-driven H^+ uptake (Dilley & Vernon, 1965; Deamer & Packer, 1969; Hind et al., 1974; Bulychev & Vredenberg, 1976; Vambutas & Schechter, 1983). Measurements with ion-selective microelectrodes in living plant cells provide evidence that approximately half of the H^+ taken up into chloroplasts after illumination are electrically compensated by Cl^- influx through putative anion channels (Thaler et al., 1992). The anion-selective ion channel measured by means of patch clamp technique in thylakoid membranes (Schönknecht et al., 1988; this study) is a possible candidate for this role. Taking this possibility as a working hypothesis, one should expect that (i) the current through the anion channels is sufficiently large to compensate at least half of the current produced by light-driven H^+ pumps; and (ii) as any ion channel contains a water-filled pore, the activity of the channels is regulated to diminish an undesirable leak of H^+ or OH^- through the open channel.

The peak currents produced by light-driven H^+ pumps in thylakoids of *Peperomia metallica* and *Amaranthus hybridus* were 200 and 40 pA, respectively, as measured by patch clamp technique (Bulychev, Antonov & Schevchenko, 1992; Muniz, Pottosin & Sandoval, 1995). Given the diameters of swollen thylakoids in these species of 30 and 13.5 μm, respectively (Schönknecht et al., 1988; Muniz et al., 1995), the peak currents above transform to 0.07 pA/μm^2. The concentration of permeant anions (Cl^- and NO_3^-; *see* Schönknecht et al., 1988) in the stroma is about 10 mM (Schröppel-Meier & Kaiser, 1988; Speer & Kaiser, 1991). So, according to our data (Fig. 10) a single-channel conductance of 30 pS can be calculated. The potential difference across the thylakoid membrane induced by a short flash or a long pulse of light transiently reaches a maximum of −20 to −80 mV (Bulychev et al., 1972, 1992; Junge & Jackson, 1982). During this transient voltage maximum a current of about −1.5 pA is carried per open anion channel. This means that one open anion channel per 20 μm^2 would be sufficient to electrically counterbalance the light-driven *net* H^+ uptake. As an average each isolated membrane patch with a surface of about 10 μm^2 contained one anion channel. This estimate shows that the current carried by the voltage-dependent anion channel is in the same order of magnitude as the maximum light-driven H^+ current.

The regulation of the activity of anion channels at steady state is the other problem to be discussed. At continuous illumination H^+ uptake by light-driven H^+ pumps and H^+ efflux through H^+-ATPases balance each other (steady state). So a membrane potential close to 0 mV is maintained without open ion channels. In this situation open ion channels even could cause some undesirable uncoupling due to a leak for H^+ or OH^-. From this point of view, the open probability for ion channels should be low at steady state and an activation should happen only when H^+ uptake and H^+ efflux are (transiently) not balanced due to light intensity changes. Any imbalance between H^+ uptake and H^+ efflux creates a transmembrane electrical potential across the thylakoid membrane that has to be balanced electrically by other ion currents. The anion channels of both *P. metallica* and *N. obtusa* thylakoids reacted correspondingly to changes of the membrane voltage. When the membrane potential was stepped e.g., to −40 mV (referring to the stromal side), which corresponds to the membrane potential after a short intense flash of light (Junge & Jackson, 1982), the anion channels opened transiently and closed again within a few seconds (Fig. 4; *cf.* Fig. 4 Schönknecht et al., 1988). Similar transient channel openings were observed when the membrane voltage was stepped to +40 mV (Fig. 4). So changes of the holding potential within the physiological range (+50 to −50 mV) elicited additional transient channel openings. Besides the rapid inactivation of the anion channel after voltage transients, other mechanisms probably contribute to a low open probability at steady state. It has been shown by Schönknecht and coworkers (1988) that the decrease of pH in the thylakoid lumen by 2 pH units had no significant effect on the Cl^- channel activity in *P. metallica* thylakoids. In this study it was demonstrated that changes of the ion concentration on the lumen side of the thylakoid membrane additionally modulate the voltage-dependent open probability (Fig. 3, bottom). When the salt concentration was decreased on the lumen side (from "100 KCl" solution to "15 KCl" solution) the open probability decreased by about a factor of two. This change was explained by a shift of both midpoint potentials V_1 and V_2 for the Boltzmann distributions describing the two gating processes of the anion channel. There are several indications that both anion uptake as well as cation release electrically compensate the light-driven *net* H^+ uptake (Dilley & Vernon, 1965; Deamer & Packer, 1969; Hind et al., 1974; Bulychev & Vredenberg, 1976). Thus, the release of cations from the thylakoid lumen may regulate the voltage-dependent anion channel and further decrease its open probability.

If the voltage-dependent anion channel has a similar behavior inside an intact leaf as described here for the isolated thylakoid membrane, then any change in the membrane voltage caused by *net* H^+ currents across the thylakoid membrane are (at least in part) electrically compensated by parallel Cl^- currents carried by the voltage-dependent anion channel. In contrast to laboratory conditions, many plants in their natural habitat are continuously confronted to light intensity changes. These light intensity changes result in imbalances between light-driven H^+ uptake and H^+ efflux causing electrogenic *net* H^+ fluxes across the thylakoid membrane. Under these conditions a proper regulated ion pathway for the electrical compensation of such electrogenic *net* H^+ fluxes is especially important.

This work was financially supported by the Deutsche Forschungsgemeinschaft (SFB 176 TP B11) and by a research fellowship from the Alexander von Humboldt Foundation to I.I. Pottosin.

References

Azzone, G., Benz, R., Bertl, A., Colombini, M., Crofts, A., Dilley, R., Dimroth, P., Dutton, P.L., Felle, H., Harold, F., Junge, W., Kaback, H.R., Knaff, D., Krulwich, T., Lodish, H., Malmström, B., Maloney, P., Mannella, C., Padan, E., Papa, S., Rottenberg, H., Rudnick, G., Rydström, J., Silverstein, T., Skulachev, V., Slayman, C., Tedeschi, H., Wikström, M., Wilson, T.H. 1993. Transmembrane measurements across bioenergetic membranes. *Biochim. Biophys. Acta* **1183**:1–3

Blatz, A.L., Magleby, K.L. 1986. Quantitative description of three modes of activity of fast chloride channels from rat sceletal muscle. *J. Physiol.* **378**:141–174

Bulychev, A.A., Andrianov, V.K., Kurella, G.A., Litvin, F.F. 1972.

Microelectrode measurements of the transmembrane potential of chloroplasts and its photoinduced changes. *Nature* **236:**175–177

Bulychev, A.A., Antonov, V.F., Schevchenko, E.V. 1992. Patch-clamp studies of light-induced currents across the thylakoid membrane of isolated chloroplasts. *Biochim. Biophys. Acta* **1099:**16–24

Bulychev, A.A., Vredenberg, W.J. 1976. Effect of ionophores A23187 and nigericin on the light-induced redistribution of Mg^{2+}, K^+, and H^+ across the thylakoid membrane. *Biochim. Biophys. Acta* **423:**548–556

Colombini, M. 1989. Voltage gating in the mitochondrial channel, VDAC. *J. Membrane Biol.* **111:**103–111

Deamer, D.W., Packer, L. 1969. Light-dependent anion transport in isolated spinach chloroplasts. *Biochim. Biophys. Acta* **172:**539–545

Dilley, R.A., Vernon, L.P. 1965. Ion and water transport processes related to the light-dependent shrinkage of spinach chloroplasts. *Arch. Biochem. Biophys.* **111:**365–375

Draber, S., Hansen, U.P. 1994. Fast single-channel measurements resolve the blocking effect of Cs^+ on the K^+ channel. *Biophys. J.* **67:**120–129

Enz, C., Steinkamp, T., Wagner, R. 1993. Ion channels in the thylakoid membrane (a patch-clamp study). *Biochim. Biophys. Acta* **1143:**67–76

Franciolini, F., Adams, D.J. 1994. Functional properties of background chloride channels. *In:* Handbook of Membrane Channels. Molecular and Cellular Physiology. C. Peracchia, editor. pp. 255–266. Academic Press, New York

Geletyuk, V.I., Kazachenko, V.N. 1985. Single Cl^- channels in molluscan neurons: Multiplicity of the conductance states. *J. Membrane Biol.* **86:**9–15

Hamill, O.P., Marty, A., Nehere, E., Sakmann, B., Sigworth, F.J. 1981. Improved patch-clamp techniques for high-resolution current recording from cells and cell-free membrane patches. *Pflüegers Arch.* **391:**85–100

Hind, G., Nakatani, H.Y., Izawa, S. 1974. Light-dependent redistribution of ions in suspensions of chloroplast thylakoid membranes. *Proc. Natl. Acad. Sci. USA* **71:**1484–1488

Junge, W., Jackson, J.B. 1982. The development of electrochemical potential gradients across photosynthetic membranes. *In:* Photosynthesis: Energy Conversion by Plants and Bacteria. Govindjee, editor. Vol. I, pp. 589–646. Academic Press, New York

Miller, C. 1982. Open-state substructure of single chloride channels from *Torpedo* electroplax. *Phil. Trans. R. Soc. Lond.* B **299:**401–411

Morier, N., Sauve, R. 1994. Analysis of a novel double-barreled anion channel from rat liver rough endoplasmic reticulum. *Biophys. J.* **67:**590–602

Muniz, J., Pottosin, I.I., Sandoval, L. 1995. Patch-clamp study of vascular plant chloroplast: single channels and photocurrents. *J. Bioenerg. Biomembr.* (*in press*)

Pottosin, I.I. 1992. Single channel recording in the chloroplast envelope. *FEBS Lett.* **308:**87–90

Pottosin, I.I., Schönknecht, G. 1995. Anion and cation channels in the thylakoid membrane. *In:* Proceedings of the Xth International Photosynthesis Congress. P. Mathis, editor. Kluwer Academic Publisher, Netherlands (*in press*)

Remiš, D., Bulychev, A.A., Kurella, G.A. 1986. The electrical and chemical components of the protonmotive force in chloroplasts as measured with capillary and pH-sensitive microelectrodes. *Biochim. Biophys. Acta* **852:**68–73

Rottenberg, H., Grunwald, T., Avron, M. 1972. Determination of ΔpH in chloroplasts 1. Distribution of [^{14}C]methylamine. *Eur. J. Biochem.* **25:**54–63

Schönknecht, G., Althoff, G., Apley, E., Wagner, R., Junge, W. 1989. Cation channels by subunit III of the channel portion of the chloroplast H^+-ATPase. *FEBS Lett.* **258:**190–194

Schönknecht, G., Hedrich, R., Junge, W., Raschke, K. 1988. A voltage-dependent chloride channel in the photosynthetic membrane of a higher plant. *Nature* **336:**589–592

Schröppel-Meier, G., Kaiser, W.M. 1988. Ion homeostasis in chloroplasts under salinity and mineral deficiency I. Solute concentrations in leaves and chloroplasts from spinach plants under NaCl or $NaNO_3$ salinity. *Plant Physiol.* **87:**822–827

Sorgato, M.C., Keller, B.U., Stühmer, W. 1987. Patch-clamping of the inner mitochondrial membrane reveals a voltage-dependent ion channel. *Nature* **330:**498–500

Sorgato, M.C., Moran, O. 1993. Channels in mitochondrial membranes: knowns, unknowns, and prospects for the future. *Critical Rev. Biochem. Mol. Biol.* **18:**127–171

Speer, M., Kaiser, W.M. 1991. Ion relations of symplastic and apoplastic space in leaves from *Spinacia oleracea* L. and *Pisum sativum* L. under salinity. *Plant Physiol.* **97:**990–997

Thaler, M., Simonis, W., Schönknecht, G. 1992. Light-dependent changes of the cytoplasmic H^+ and Cl^- activity in the green alga *Eremosphaera viridis*. *Plant Physiol.* **99:**103–110

Tester, M., Blatt, M.R. 1989. Direct measurement of K^+ channels in thylakoid membranes by incorporation of vesicles into planar lipid bilayers. *Plant Physiol.* **91:**249–252

Vambutas, V., Schechter, S. 1983. Chloride ion transport and its inhibition in thylakoid membranes. *Arch. Biochem. Biophys.* **224:**442–448

White, M.M., Miller, C. 1979. A voltage-dependent anion channel from the electric organ of *Torpedo californica*. *J. Biol. Chem.* **254:** 10161–10166